Astron. & Astrophys. 41, 27–36 (1975)

Optical Study of the Carina Nebula*

L. Deharveng and M. Maucherat
Observatoire de Marseille, Laboratoire d'Astronomie Spatiale du CNRS

Received December 27, 1974

Summary. We present monochromatic photographs in Hβ, [O III] λ 5007, Hα, [N II] λ 6584, [S II] λλ 6717–6731, of two peculiar regions of the Carina Nebula: a bright circular ring around the radio peak Car II, and bright rims near Car I. They show small scale structure and steep variations in the ionization conditions.
A kinematical study of the Nebula is obtained with interference techniques and high angular and spectral resolution in Hα and [N II]. This confirms the existence of a general expansion of the nebula, with non-spherical symmetry. The expansion velocity of the ionized gas is $\geqslant 25$ km s^{-1} although that of the neutral surrounding gas is much smaller.

Key words: H II region — ionization — kinematics

I. Introduction

The great Carina Nebula is one of the brightest nebulae of the southern Milky Way. It is an object of great interest: it contains strong radio sources, and several star clusters including Trumpler 14 and 16 which contain extremely early O stars and Wolf-Rayet stars (Walborn, 1971, 1973). Two prominent dust lanes, bordered by bright rims, cross the nebula. Infra-red emission (Hoffman *et al.*, 1973) comes from these regions. OH and H_2CO molecules as well as neutral gas seem to be associated with the obscuring dust (Dickel and Wall, 1974; Dickel, 1974).
Figure 1b shows the part of the Carina Nebula studied in this paper, between the two conspicuous absorption lanes. This region is of high excitation (Faulkner, 1963, 1965), and covers the two strong radio sources Car I and Car II[1]) (Gardner and Morimoto, 1968; Shaver and Goss, 1970; Gardner *et al.*, 1970).
Unusual kinematical behavior has been found inside this region, from the broadening—and sometimes splitting—of the radio recombination lines, especially in the vicinity of Car II (McGee and Gardner, 1968, for the H 126α line; McGee *et al.*, 1969, for the H 158α line; Wilson *et al.*, 1970, for the H 109α line). Previous optical observations of the gas velocity (Georgelin, 1969; Smith, 1970) confirm the existence of large movements near Car II.
New observations with interference techniques and higher angular and spectral resolution are presented here.

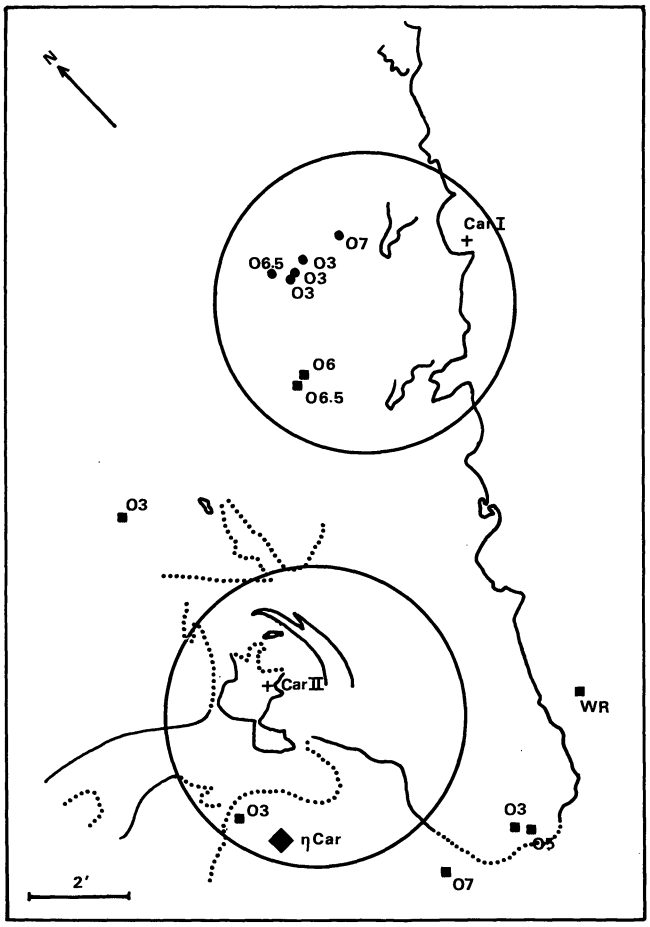

Fig. 1a. Chart showing the observed part of the Carina Nebula (field of Fig. 2). The two circles limit the fields of Figs. 3 and 4. The stars of Trumpler 14 are marked by dots, those of Trumpler 16 by squares; their spectral type is from Walborn (1973)

* Observations were made at the European Southern Observatory.
[1]) Car I = *G* 287.4–0.6, $\alpha_{1950} = 10^h41^m36^s$, $\delta_{1950} = -59°19'$: Car II = *G* 287.6–0.6, $\alpha_{1950} = 10^h42^m50^s$, $\delta_{1950} = -59°23.0$ (Gardner *et al.*, 1970).

Fig. 1b. Reproduction of an ESO plate (1 m Schmidt telescope; IIaO kodak emulsion, GG 385 filter, exposure time 60^m)

II. Monochromatic Photographs

Several monochromatic photographs of the Carina Nebula were taken in April 1971 and January 1972 at the European Southern Observatory at La Silla in Chile. The device used is the "*focal reducer*" described by Courtès (1960), mounted at the Cassegrain focus of the 152 cm telescope; the exceptional brightness of the Carina Nebula has enabled us to use an aperture ratio of $F/2.9$, which gives a photographic plate scale of 47″/mm. The photographs were taken through narrow interference filters centered on the following emission lines: Hβ, [O III] λ 5007, Hα, [N II] λ 6584, [S II] $\lambda\lambda$ 6717–6731. The bandwidths at half-maximum transmission were about 10 Å, with the exception of the [S II] filter which had a width of 50 Å, and a second Hα filter of 25 Å.

Figure 2 is an Hα photograph of the studied region. It shows a complex structure and great brightness inhomogeneities. Several bright rims, one of which coin-

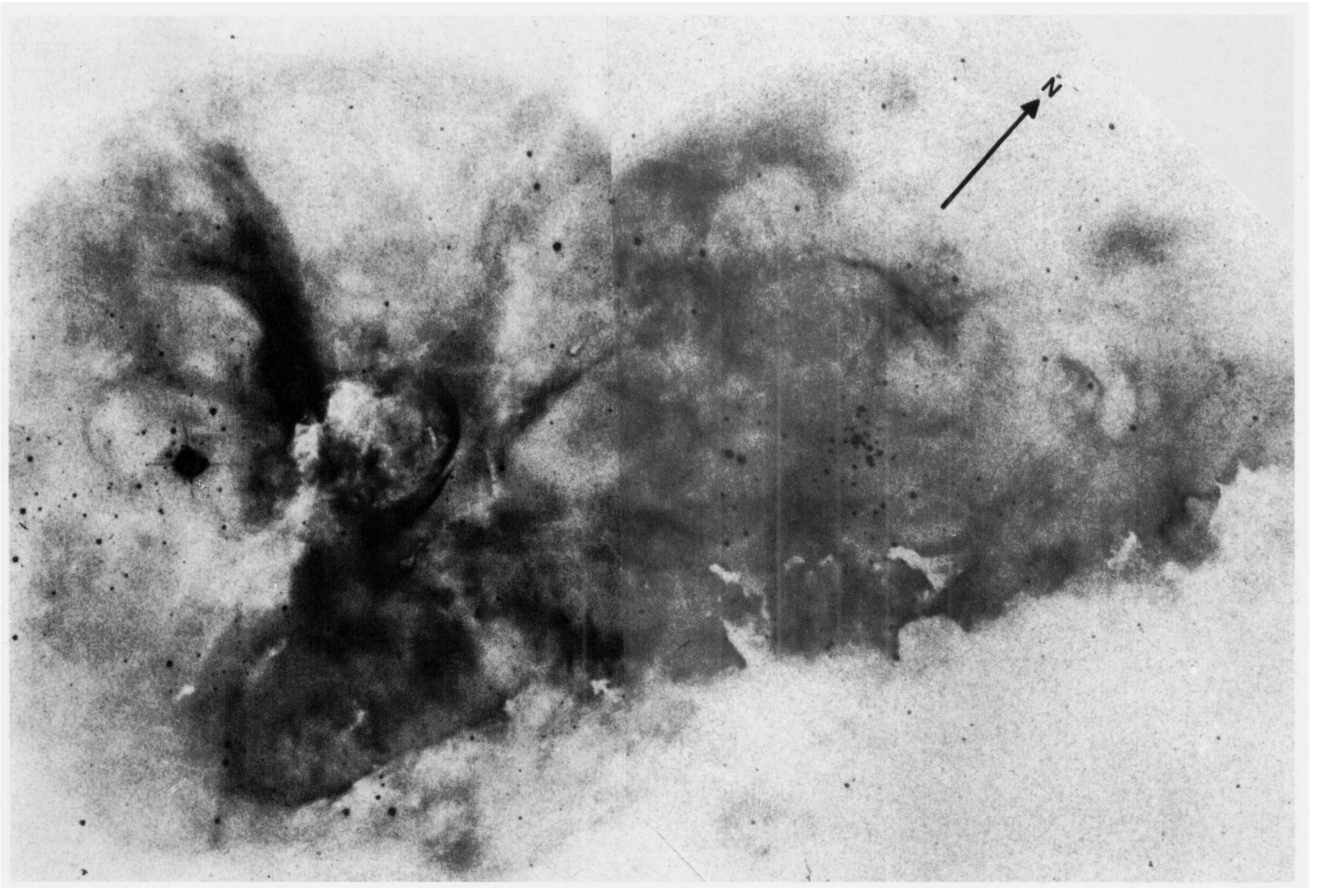

Fig. 2. Composition of two Hα photographs ($\Delta\lambda = 25$ Å, exposure time 5^m)

cides with the radio peak Car I (Gardner *et al.*, 1970), and "*elephant trunks*" are located on the edges of the northwest absorption lane. About 4′ northwest of the star η Carinae is an almost circular ring of nebulosity, about 3′ in diameter, the center of which coincides with the radio peak Car II (Gardner *et al.*, 1970). Several bands of enhanced emission start from the ring; a patch of absorption to the south extends somewhat into the ring.

It is difficult to find the exciting stars of the nebula. Each cluster, Trumpler 14 and Trumpler 16, contains extremely early O stars which can excite the nebula. Walborn (1973) thinks that only Trumpler 16 ($D \sim$ 2600 pc) is associated with the Carina Nebula. The fact that most of the well-defined "*elephant trunks*" point to the south-east of the nebula would seem to confirm this (Trumpler 14 is north-west of the nebula). They could point either to the peculiar star η Carinae (given by Pottasch, 1956, with a false HD number, as the exciting star of the bright rims), or to the nearby O 3 star HD 303308 (Walborn, 1973). But they could also point to the bright ring nebulosity: Walborn (1973) underlined that this structure is located within an area in which no O stars are yet known, but where a heavily obscured high-luminosity star could be hidden. The presence of four globules near the ring structure reveals the proximity of the exciting stars (Pottasch, 1956).

Figures 3 and 4 show monochromatic photographs (Hβ, [O III], [N II], [S II]) of two interesting regions: the bright circular ring around Car II, and the bright rims near Car I. Each of these regions presents the same appearance, on the one hand in [N II] and [S II], and on the other hand in Hα, Hβ and [O III]. This can be attributed to the ionization structure: [N II] and [S II] are emitted by low-excitation regions, [O III] by high-excitation ones. As this part of the nebula is, as a whole, of high excitation (Faulkner, 1963), there are many O^{++} and few O^{+} ions, so the appearance is the same in Hα, Hβ and [O III]. Bright rims, globules, and the ring of nebulosity are enhanced on the [N II] and [S II] photographs. They appear as regions of lower excitation than the surrounding nebulosity (this is confirmed by the absence of [O III] emission at the bright rims). These structures probably border dense regions of neutral gas, as is known to be the case for bright rims and globules (Pottasch, 1965). These features have also been discussed by Smith (1972).

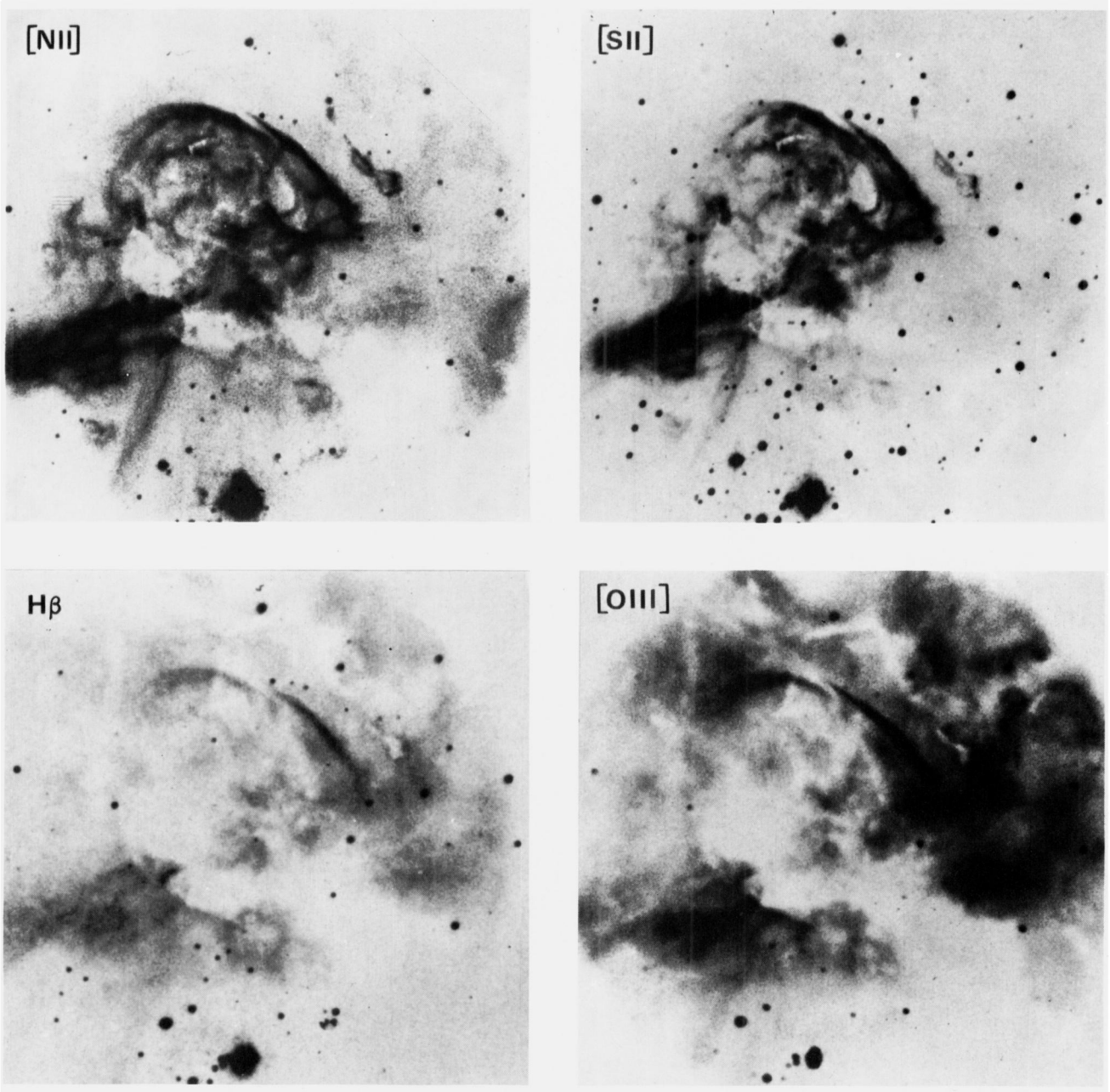

Fig. 3. [N II] photograph—exposure time 50^m, [S II] photograph—exposure time 30^m, Hβ photograph—exposure time 30^m, [O III] photograph—exposure time 15^m

III. Kinematical Study

III.1. Observations

Several interferograms in Hα and [N II] (λ 6584) were taken with the same device used for monochromatic photographs. Figure 1b shows the field covered by these interferograms. Observational data can be found in Table 1. The aperture ratio of $F/2.9$ gives a good angular resolution (photographic plate scale of 47″/mm) and a high accuracy for radial velocities. Some interferograms were taken in [N II]; because of its smaller temperature broadening, the perturbations of its profile due to internal motions are easier to detect than in the Hα interferograms.

III.2. Results

The most important feature is the splitting of Hα and [N II] on all interferograms. Figure 5 shows a striking example of splitting in Hα, in the vicinity of the star η Carinae and of the radio emission peak Car II.

Table 2 gives the radial velocities obtained from Hα for 689 points in the nebula. A comparison of nearly coincident regions on the three Hα interferograms in-

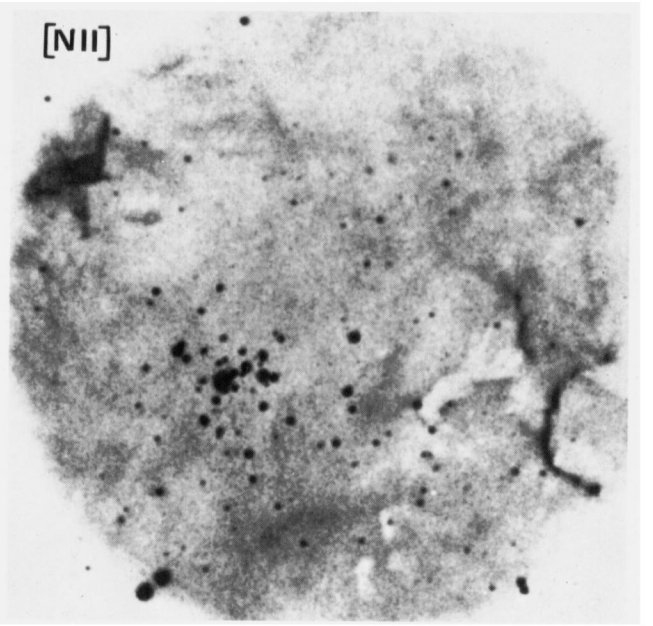

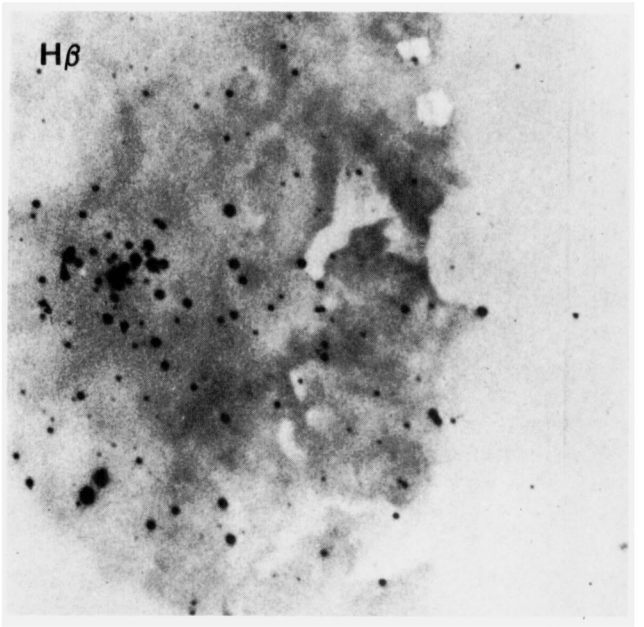

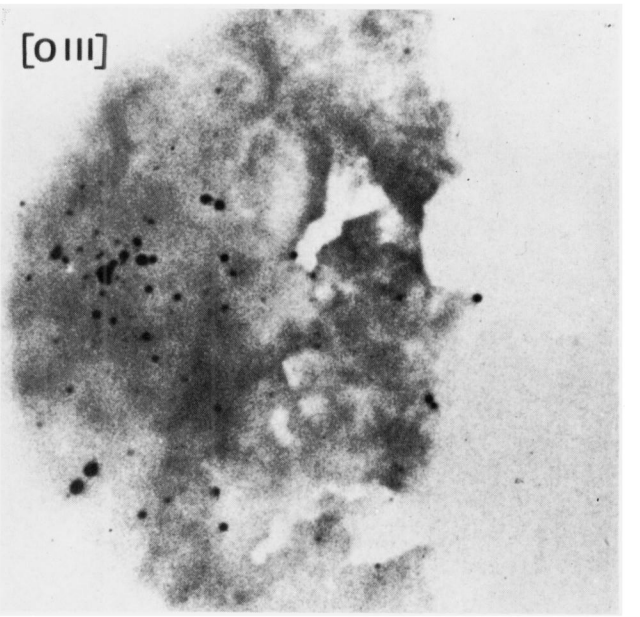

Fig. 4. [N II] photograph—exposure time 50^m, $H\beta$ photograph—exposure time 1^h, [O III] photograph—exposure time 30^m

Table 1. Basic data relating to the observations

Interferogram, identification number	Exposure time	Observed line	Interference order	Finesse	Dispersion at the first ring	Mean dispersion for the place
× 243	50^m	Hα	1360	15	2.9 Å/mm	7 Å/mm
× 244	1^h	Hα	1360	15	2.9 Å/mm	7 Å/mm
× 248	1^h	Hα	1360	15	2.9 Å/mm	7 Å/mm
× 238	5^h	[N II]	4770	14	1.6 Å/mm	3 Å/mm
× 267	4^h19^m	[N II]	4770	14	1.6 Å/mm	3 Å/mm

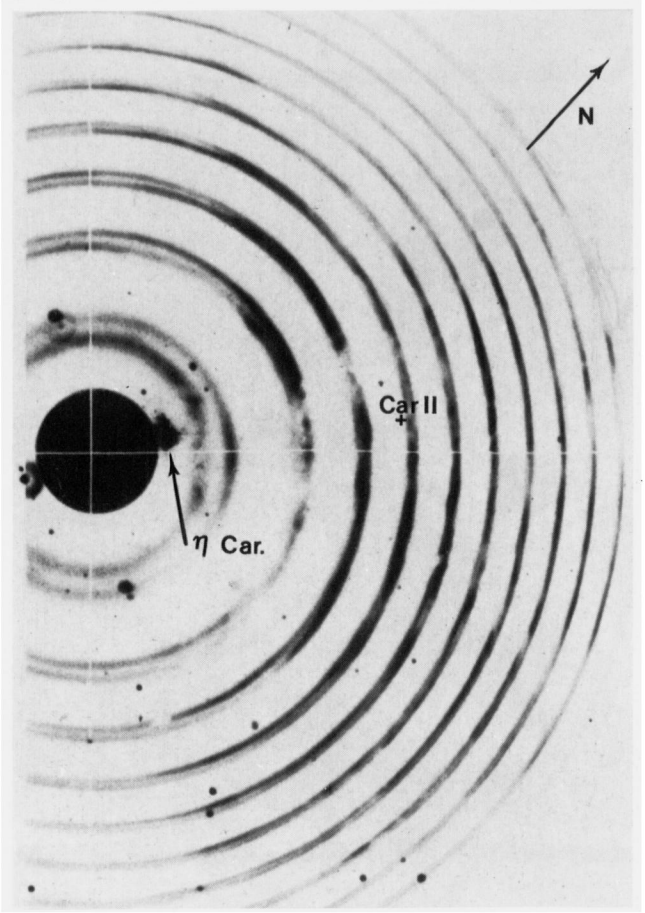

Fig. 5. Hα interferogram number X 243

dicates a standard deviation of $\pm 1.8\,\mathrm{km\,s^{-1}}$ for a single measure. The coordinates are given with an accuracy of about $\pm 3''$. Because of the spectrographic method employed in our work, the two components of a split line are not measured precisely at the same point in the nebula. The two components, in cases of splitting, are referenced with a common number in Column 4.

Table 3 gives the relative radial velocities obtained from [N II]. Owing to the lack of precision of the standard [N II] wavelength, these velocities are obtained to within an unknown additive constant only.

III.3. Discussion

We have compared the radial velocities obtained by Gardner *et al.* (1970) from the H 109α line (4′ beam), with a mean optical velocity calculated for the same resolution. This comparison is possible only for regions of homogeneous brightness (positions J and G of Gardner *et al.*, 1970) and shows good agreement between the two determinations of the velocity:

$$\begin{cases}\text{Position G: } V_{\text{radio}} = -17.6\,\mathrm{km\,s^{-1}},\ V_{\text{opt}} = -19.6\,\mathrm{km\,s^{-1}},\\ \text{Position J: } V_{\text{radio}} = -20.8\,\mathrm{km\,s^{-1}},\ V_{\text{opt}} = -19.7\,\mathrm{km\,s^{-1}}.\end{cases}$$

The splitting of Hα and [N II], which appears on all interferograms, occurs over extended regions of the nebula (Fig. 5). Figure 6 shows the radial velocity differences between the two components of the line, for those points exhibiting Hα line splitting. The strongest splitting (radial velocity difference of more than $50\,\mathrm{km\,s^{-1}}$) is observed in close proximity to the star η Carinae. Strong splitting (40 to $50\,\mathrm{km\,s^{-1}}$) is also observed near η Carinae both in the obscured region and in the bright nebulosity. Figure 6 shows that the splitting is observed over distances of more than 14′, equivalent to 11 pc assuming the distance to the Carina Nebula to be 2.7 kpc (Sher, 1965). No splitting was found in the northern part of our observed region, nor in the north-west absorbing lane.

All these results are in very good agreement with the H 109α line profiles observed by Gardner *et al.* (1970), who find large line splitting near the radio peak Car II and the star η Carinae, and no splitting near the radio peak Car I, in the north-west part of the nebula.

Furthermore, there seems to be no correlation between the splitting and the optical structure of the nebula except, as we shall see below, for the circular ring of nebulosity north of η Carinae (Fig. 3).

Significant line splitting is found on [N II] interferograms taken on the circular ring structure (Fig. 3). Figure 7 shows the radial velocity differences between the two components of this line. A correlation seems to exist between the optical structure and the splitting. Strong splitting (more than $40\,\mathrm{km\,s^{-1}}$), is observed near the center of the ring. Similarly strong splitting is also observed to the south-east of the ring, on each side of the absorption patch. No splitting is found on the steep edge west of the ring; there the velocity is a mean between those of each component. These results can be interpreted as an expansion of the ring with a speed of about $21\,\mathrm{km\,s^{-1}}$.

Within the ring, the radial velocity differences between the two components of Hα and [N II] are in good agreement. Outside, in some places (Fig. 7), only one component is observed for [N II] while two are observed for Hα. Where Hα splitting is observed the [N II] velocity corresponds to the velocity of one component of Hα. Thus we observe two clouds of distinct velocities emitting Hα and only one, receding or approaching, emitting [N II]. These two clouds must be in different states of ionization (one of low excitation emitting Hα and [N II], the other of high excitation emitting Hα and [O III]). In confirmation of this interpretation, we note that this type of splitting occurs in a region for which the structure appears quite different in [N II] and in [O III] (Fig. 3).

The splitting occurs over very extended regions of the Nebula (more than 11 pc). Such a phenomenon was found in the Orion Nebula (Deharveng, 1973), but on a smaller scale (about 1 pc). For the Orion Nebula we already showed that such a splitting could not be ex-

e 2. Radial velocities V_{LSR} obtained from Hα

α_{1950}	δ_{1950}	V_{LSR} km/s	I
10 40 47.7	-59 10 23	-16.0	
10 40 49.6	-59 10 43	-17.2	
10 40 51.6	-59 11 3	-16.7	
10 40 53.7	-59 11 24	-20.7	
10 40 55.2	-59 9 47	-15.8	
10 40 55.9	-59 11 48	-19.8	
10 40 56.7	-59 10 8	-19.2	
10 40 58.2	-59 10 31	-19.8	
10 40 58.4	-59 12 14	-21.3	
10 40 59.8	-59 10 55	-21.3	
10 41 1.2	-59 12 42	-21.7	
10 41 1.6	-59 11 21	-19.7	
10 41 3.6	-59 11 49	-19.5	
10 41 4.4	-59 13 15	-22.2	
10 41 5.7	-59 12 21	-22.3	
10 41 6.3	-59 9 38	-23.5	
10 41 7.2	-59 10 2	-26.0	
10 41 8.2	-59 12 57	-21.5	
10 41 8.3	-59 13 55	-21.3	
10 41 8.3	-59 10 29	-22.7	
10 41 9.4	-59 10 57	-22.7	
10 41 10.6	-59 11 27	-23.8	
10 41 11.3	-59 13 42	-22.2	
10 41 11.9	-59 12 2	-22.3	
10 41 13.5	-59 12 42	-18.7	
10 41 15.3	-59 13 29	-22.0	
10 41 15.7	-59 14 45	-24.0	
10 41 18.0	-59 14 38	-22.8	
10 41 18.3	-59 9 22	-21.0	
10 41 18.5	-59 9 48	-21.0	
10 41 18.7	-59 10 15	-21.5	
10 41 19.0	-59 10 44	-20.8	
10 41 19.2	-59 11 16	-21.0	
10 41 19.6	-59 11 52	-21.3	
10 41 19.9	-59 12 32	-24.3	
10 41 20.4	-59 13 26	-11.1	
10 41 21.0	-59 14 35	-21.5	
10 41 23.4	-59 14 37	-19.7	
10 41 23.6	-59 14 19	-19.8	
10 41 24.6	-59 13 26	-15.5	
10 41 25.1	-59 14 40	-20.1	
10 41 25.4	-59 12 35	-16.0	
10 41 26.0	-59 14 41	-20.3	
10 41 26.1	-59 11 54	-17.7	
10 41 26.7	-59 15 2	-21.1	
10 41 26.7	-59 11 18	-16.2	
10 41 27.2	-59 10 46	-14.8	
10 41 28.3	-59 15 26	-23.1	
10 41 28.7	-59 14 50	-20.3	
10 41 29.1	-59 13 34	-14.4	
10 41 30.2	-59 15 52	-23.8	
10 41 30.3	-59 17 41	-23.7	
10 41 30.3	-59 15 0	-20.2	
10 41 31.3	-59 12 46	-15.5	
10 41 31.7	-59 17 28	-20.8	
10 41 32.2	-59 16 20	-21.3	
10 41 32.4	-59 15 16	-20.7	
10 41 32.8	-59 17 18	-19.5	
10 41 32.9	-59 13 48	-14.1	
10 41 33.0	-59 12 7	-12.4	
10 41 33.5	-59 13 51	-11.1	
10 41 33.6	-59 15 28	-23.8	
10 41 33.9	-59 14 11	-14.2	
10 41 34.0	-59 17 3	-22.0	
10 41 34.4	-59 16 52	-22.2	
10 41 34.5	-59 11 34	-10.6	
10 41 34.7	-59 16 51	-23.2	
10 41 34.7	-59 15 49	-22.0	
10 41 34.9	-59 14 35	-16.9	
10 41 35.0	-59 16 40	-22.0	
10 41 35.1	-59 16 21	-19.3	
10 41 35.1	-59 16 8	-20.0	
10 41 35.9	-59 11 3	-11.9	
10 41 36.0	-59 18 39	-26.8	
10 41 36.1	-59 15 1	-18.1	
10 41 36.4	-59 14 6	-13.5	
10 41 37.0	-59 17 28	-18.6	
10 41 37.1	-59 13 8	-8.3	
10 41 37.3	-59 15 28	-20.7	
10 41 38.4	-59 18 18	-15.5	
10 41 38.6	-59 15 59	-20.3	
10 41 39.8	-59 19 18	-20.2	
10 41 40.0	-59 12 33	-10.5	
10 41 40.1	-59 18 12	-22.5	
10 41 40.1	-59 16 33	-19.8	
10 41 40.1	-59 14 35	-18.0	
10 41 40.5	-59 18 2	-23.2	
10 41 40.9	-59 13 27	-19.8	
10 41 41.8	-59 17 13	-15.9	
10 41 41.9	-59 14 56	-18.0	
10 41 42.5	-59 12 2	-12.0	
10 41 43.1	-59 19 52	-23.0	
10 41 43.2	-59 18 53	-15.3	
10 41 43.2	-59 17 15	-13.9	
10 41 43.2	-59 13 29	-18.4	
10 41 43.6	-59 15 31	-14.4	
10 41 43.6	-59 13 53	-18.2	
10 41 43.9	-59 16 58	-15.5	
10 41 44.1	-59 14 19	-13.2	
10 41 44.4	-59 16 27	-13.7	
10 41 44.4	-59 12 56	-17.2	
10 41 44.5	-59 16 4	-16.5	
10 41 44.6	-59 14 46	-13.4	
10 41 44.7	-59 19 18	-17.9	
10 41 44.7	-59 11 35	-11.2	
10 41 45.1	-59 15 15	-14.4	
10 41 45.2	-59 14 7	-7.1	
10 41 45.6	-59 18 32	-18.2	
10 41 45.7	-59 15 47	-13.6	
10 41 46.0	-59 20 21	-25.2	
10 41 46.4	-59 16 23	-13.9	
10 41 46.7	-59 11 10	-11.9	
10 41 46.9	-59 19 10	-18.2	
10 41 47.1	-59 17 3	-19.1	
10 41 47.2	-59 19 23	-19.3	
10 41 47.4	-59 12 29	-17.2	
10 41 47.8	-59 14 33	-21.7	
10 41 48.1	-59 17 59	-15.2	
10 41 48.1	-59 17 55	-12.2	
10 41 48.5	-59 20 46	-22.0	
10 41 48.7	-59 10 46	-17.5	
10 41 49.3	-59 19 4	-23.5	
10 41 49.5	-59 17 33	-13.7	
10 41 49.7	-59 13 42	-8.5	
10 41 49.9	-59 18 57	-16.8	
10 41 49.9	-59 15 19	-9.1	
10 41 50.2	-59 17 11	-8.9	
10 41 50.2	-59 12 5	-14.3	
10 41 50.6	-59 19 48	-24.3	
10 41 50.8	-59 16 30	-6.2	1
10 41 50.8	-59 16 1	-7.3	
10 41 51.5	-59 16 30	-28.9	1
10 41 52.4	-59 19 6	-15.7	
10 41 52.5	-59 14 15	-13.3	
10 41 52.8	-59 11 42	-20.5	
10 41 52.9	-59 21 31	-20.2	
10 41 53.0	-59 18 19	-21.5	
10 41 53.3	-59 17 52	-17.2	
10 41 53.6	-59 20 10	-22.3	
10 41 53.6	-59 13 21	-10.5	
10 41 53.8	-59 19 19	-24.3	
10 41 53.9	-59 17 2	-16.2	
10 41 54.3	-59 16 23	-5.7	
10 41 54.5	-59 17 47	-9.4	2
10 41 54.7	-59 15 46	-6.8	
10 41 54.9	-59 21 52	-22.8	
10 41 55.0	-59 17 48	-30.2	2
10 41 55.1	-59 15 14	-10.1	
10 41 55.1	-59 11 22	-17.2	
10 41 55.2	-59 19 7	-23.2	
10 41 55.2	-59 15 9	-9.7	
10 41 55.4	-59 14 44	-12.8	
10 41 55.7	-59 17 22	-18.8	
10 41 55.8	-59 14 17	-14.2	
10 41 56.0	-59 13 51	-13.0	
10 41 56.3	-59 16 33	-8.2	3
10 41 56.3	-59 15 58	-7.4	
10 41 56.3	-59 13 27	-12.9	
10 41 56.4	-59 20 31	-23.3	
10 41 56.6	-59 13 58	-12.0	
10 41 56.8	-59 22 12	-24.5	
10 41 56.9	-59 16 33	-32.7	3
10 41 57.1	-59 19 39	-23.0	
10 41 57.1	-59 13 2	-15.5	
10 41 57.2	-59 18 36	-22.0	
10 41 57.8	-59 17 58	-23.1	
10 41 58.0	-59 19 15	-25.4	
10 41 58.3	-59 22 13	-19.3	
10 41 58.9	-59 20 50	-18.5	
10 41 59.2	-59 18 0	-23.5	
10 41 59.5	-59 17 13	-5.9	4
10 41 59.7	-59 17 7	-35.4	4
10 41 59.7	-59 15 0	-9.9	
10 42 0.0	-59 22 5	-21.5	
10 42 0.0	-59 17 30	-6.1	5
10 42 .1	-59 19 56	-22.5	
10 42 .3	-59 19 27	-27.5	
10 42 .5	-59 17 31	-31.3	5
10 42 .5	-59 13 43	-18.0	
10 42 .9	-59 18 51	-21.5	
10 42 1.0	-59 16 32	-8.3	6
10 42 1.0	-59 15 56	-5.9	
10 42 1.1	-59 16 36	-9.3	7
10 42 1.2	-59 16 29	-29.3	6
10 42 1.3	-59 21 7	-16.3	
10 42 1.5	-59 21 55	-22.8	
10 42 1.5	-59 16 36	-31.2	7
10 42 2.1	-59 19 43	-24.6	
10 42 2.2	-59 18 16	-10.1	8
10 42 2.3	-59 15 58	-4.9	
10 42 2.5	-59 21 46	-25.0	
10 42 2.5	-59 18 11	-30.6	8
10 42 3.1	-59 20 13	-26.5	
10 42 3.1	-59 18 11	-19.8	
10 42 3.4	-59 23 13	-14.4	
10 42 3.5	-59 15 27	-6.4	
10 42 3.6	-59 21 32	-25.5	
10 42 3.6	-59 21 25	-25.8	
10 42 3.7	-59 20 1	-26.1	
10 42 3.8	-59 14 51	-8.8	
10 42 3.8	-59 13 30	-12.0	
10 42 4.1	-59 17 38	-4.0	9
10 42 4.3	-59 21 1	-16.6	
10 42 4.3	-59 20 12	-27.1	
10 42 4.3	-59 19 4	-16.8	
10 42 4.6	-59 21 17	-29.2	
10 42 4.6	-59 17 40	-35.8	9
10 42 4.6	-59 14 58	-11.2	
10 42 4.7	-59 20 33	-23.5	
10 42 5.0	-59 20 45	-26.6	
10 42 5.2	-59 16 38	-7.0	10
10 42 5.3	-59 17 32	-3.6	11
10 42 5.4	-59 15 54	-17.2	
10 42 5.6	-59 14 31	-13.2	
10 42 5.7	-59 20 29	-27.8	
10 42 5.7	-59 17 26	-35.2	11
10 42 5.8	-59 16 38	-37.4	10
10 42 5.9	-59 18 36	-7.7	12
10 42 6.3	-59 23 0	-22.0	
10 42 6.5	-59 18 31	-34.7	12
10 42 6.6	-59 18 21	-11.2	13
10 42 6.6	-59 14 5	-19.1	
10 42 6.9	-59 18 22	-33.7	13
10 42 7.2	-59 23 58	-24.7	
10 42 7.3	-59 19 16	-6.5	14
10 42 7.4	-59 13 44	-13.7	
10 42 7.6	-59 14 44	-11.2	
10 42 7.7	-59 19 18	-39.9	14
10 42 7.8	-59 17 46	-2.9	15
10 42 7.9	-59 16 55	-5.7	16
10 42 8.2	-59 20 43	-25.7	
10 42 8.3	-59 17 47	-33.3	15
10 42 8.3	-59 16 50	-35.2	16
10 42 8.8	-59 22 42	-25.0	
10 42 8.9	-59 19 1	-5.3	17
10 42 9.1	-59 16 40	-9.8	18
10 42 9.2	-59 15 53	-14.7	
10 42 9.6	-59 16 40	-35.5	18
10 42 9.8	-59 18 55	-39.2	17
10 42 9.9	-59 18 30	-8.3	19
10 42 10.1	-59 19 28	1.7	20
10 42 10.2	-59 17 57	-5.6	21
10 42 10.3	-59 24 34	-34.8	
10 42 10.3	-59 18 32	-38.3	19
10 42 10.3	-59 16 22	-13.2	
10 42 10.4	-59 22 27	-27.9	
10 42 10.7	-59 23 37	-22.0	
10 42 10.7	-59 19 30	-41.3	20
10 42 10.8	-59 17 52	-37.9	21
10 42 11.1	-59 14 37	-14.4	
10 42 11.3	-59 19 32	-3.4	22
10 42 11.3	-59 17 53	-3.1	23
10 42 11.8	-59 17 54	-35.5	23
10 42 12.3	-59 22 1	-29.8	
10 42 12.3	-59 19 49	-4.1	24
10 42 12.3	-59 15 53	-16.1	
10 42 12.4	-59 18 48	3.8	
10 42 12.5	-59 19 27	-40.2	22
10 42 12.7	-59 16 42	-7.2	
10 42 12.8	-59 15 51	-16.5	
10 42 12.9	-59 25 4	-36.3	
10 42 13.0	-59 19 39	-3.9	
10 42 13.0	-59 18 39	-8.4	25
10 42 13.3	-59 20 22	-1.1	26
10 42 13.4	-59 18 40	-33.5	25
10 42 13.5	-59 19 46	-39.2	24
10 42 13.6	-59 21 36	-31.1	
10 42 13.6	-59 20 42	-2.5	27
10 42 13.7	-59 17 24	-8.2	
10 42 14.1	-59 23 15	-37.8	
10 42 14.1	-59 18 28	-6.1	28
10 42 14.1	-59 15 27	-17.4	
10 42 14.2	-59 27 24	4.1	
10 42 14.3	-59 14 31	-10.9	
10 42 14.4	-59 21 10	-32.3	
10 42 14.4	-59 20 20	-35.2	26
10 42 14.5	-59 24 10	-37.4	
10 42 14.6	-59 24 20	-41.2	
10 42 14.6	-59 20 42	-33.7	27
10 42 14.6	-59 17 59	-5.2	
10 42 14.8	-59 18 24	-41.3	28
10 42 14.9	-59 25 28	-10.6	29
10 42 15.2	-59 25 31	-35.9	29
10 42 15.8	-59 15 3	-14.4	
10 42 16.0	-59 22 55	-31.9	
10 42 16.0	-59 18 47	-4.5	
10 42 16.0	-59 16 44	-7.7	
10 42 16.1	-59 15 49	-17.0	
10 42 16.2	-59 25 31	-39.1	30
10 42 16.6	-59 25 31	-14.5	30
10 42 16.7	-59 16 57	-7.7	
10 42 17.0	-59 25 52	-9.7	31
10 42 17.2	-59 24 33	-6.2	32
10 42 17.3	-59 25 55	-36.4	31
10 42 17.4	-59 19 8	-4.4	33
10 42 17.4	-59 14 41	-14.9	
10 42 17.6	-59 24 26	-41.5	34
10 42 17.7	-59 24 38	-43.9	32
10 42 17.7	-59 18 5	-11.7	
10 42 18.1	-59 24 27	-6.1	34
10 42 18.3	-59 23 41	-38.9	
10 42 18.3	-59 19 4	-42.9	33
10 42 18.4	-59 18 1	-10.9	
10 42 18.5	-59 22 22	-34.3	
10 42 18.7	-59 19 31	-4.4	35
10 42 19.0	-59 26 15	-6.8	36
10 42 19.2	-59 26 18	-34.9	36
10 42 19.2	-59 16 45	-5.8	
10 42 19.2	-59 15 48	-13.9	
10 42 19.3	-59 19 48	-2.5	37
10 42 19.4	-59 19 29	-34.3	35
10 42 19.5	-59 16 32	-10.5	
10 42 19.6	-59 26 43	-39.1	38
10 42 19.6	-59 25 33	-37.0	39
10 42 19.9	-59 20 13	2.3	40
10 42 20.0	-59 26 42	-8.7	38
10 42 20.0	-59 25 34	-10.1	39
10 42 20.0	-59 24 58	-8.6	41
10 42 20.1	-59 21 49	-34.4	
10 42 20.2	-59 20 40	2.3	42
10 42 20.2	-59 19 46	-37.1	37
10 42 20.4	-59 25 1	-37.7	41
10 42 20.5	-59 23 23	-34.1	
10 42 20.5	-59 23 18	-34.8	
10 42 20.7	-59 28 52	-20.4	
10 42 20.8	-59 24 32	-43.7	43
10 42 20.9	-59 26 37	-16.4	44
10 42 21.0	-59 26 39	-37.1	44
10 42 21.0	-59 21 15	-36.6	
10 42 21.0	-59 20 12	-39.4	40
10 42 21.3	-59 24 33	-9.9	43
10 42 21.3	-59 20 40	-38.2	42
10 42 21.4	-59 27 43	-8.5	
10 42 21.8	-59 24 4	-37.3	
10 42 22.0	-59 16 9	-13.2	
10 42 22.1	-59 17 38	-14.4	
10 42 22.2	-59 18 49	-4.2	
10 42 22.4	-59 22 5	4.1	
10 42 22.6	-59 26 57	-11.4	45
10 42 22.7	-59 25 21	-19.1	
10 42 22.8	-59 27 0	-42.1	45
10 42 23.1	-59 26 40	-38.9	46
10 42 23.1	-59 25 36	-35.0	47
10 42 23.2	-59 22 38	-28.8	
10 42 23.5	-59 26 40	-13.5	46
10 42 23.5	-59 25 36	-11.5	47
10 42 23.6	-59 23 33	-32.0	
10 42 23.8	-59 19 17	-4.4	48
10 42 24.1	-59 27 16	-3.7	
10 42 24.3	-59 27 37	-39.6	49
10 42 24.3	-59 23 37	-31.1	
10 42 24.3	-59 15 48	-13.2	
10 42 24.5	-59 19 15	-36.6	48
10 42 24.6	-59 24 39	-20.5	
10 42 24.6	-59 24 22	-8.5	50
10 42 24.6	-59 19 36	-4.4	51
10 42 24.8	-59 27 35	-9.2	49
10 42 25.0	-59 25 40	-8.5	52
10 42 25.1	-59 24 25	-41.4	50
10 42 25.1	-59 22 19	-30.1	
10 42 25.1	-59 21 59	-29.9	
10 42 25.3	-59 25 43	-42.9	52
10 42 25.3	-59 19 35	-36.1	51
10 42 25.4	-59 20 6	-.6	53
10 42 25.4	-59 17 18	-15.2	
10 42 25.7	-59 20 38	1.6	54
10 42 26.2	-59 20 5	-37.1	53
10 42 26.3	-59 21 20	-34.9	
10 42 26.4	-59 18 32	-4.9	
10 42 26.4	-59 15 28	-14.1	
10 42 26.7	-59 20 38	-41.3	54
10 42 26.8	-59 28 33	-39.1	55
10 42 26.8	-59 25 38	-42.0	56
10 42 26.8	-59 23 43	-35.2	
10 42 27.2	-59 26 0	-10.4	57
10 42 27.3	-59 28 31	-2.1	55
10 42 27.4	-59 26 37	-8.5	
10 42 27.4	-59 25 38	-10.9	56
10 42 27.4	-59 22 53	-23.6	
10 42 27.6	-59 26 3	-44.2	57
10 42 27.6	-59 24 41	-9.9	
10 42 27.9	-59 24 45	-46.0	58
10 42 27.9	-59 23 55	-33.4	
10 42 27.9	-59 22 33	-24.7	
10 42 28.1	-59 27 30	-39.6	59
10 42 28.2	-59 29 42	-12.4	
10 42 28.2	-59 19 4	-4.4	60
10 42 28.4	-59 16 59	-15.2	
10 42 28.4	-59 15 10	-13.2	
10 42 28.5	-59 24 46	-10.5	58
10 42 28.6	-59 27 29	-10.9	59
10 42 28.8	-59 19 2	-35.3	60
10 42 29.2	-59 19 26	-4.2	61
10 42 29.3	-59 26 18	-8.3	62
10 42 29.6	-59 26 20	-44.2	62
10 42 29.6	-59 22 8	-28.8	
10 42 29.8	-59 19 25	-39.3	61
10 42 30.0	-59 20 0	-.7	63
10 42 30.3	-59 28 21	-39.5	64
10 42 30.3	-59 18 17	-11.2	
10 42 30.4	-59 24 58	-8.3	65
10 42 30.4	-59 23 55	-31.7	
10 42 30.5	-59 20 36	-.1	66
10 42 30.7	-59 25 0	-38.2	65
10 42 30.8	-59 29 30	-41.2	67
10 42 30.8	-59 28 19	-6.2	64
10 42 30.8	-59 19 59	-37.4	63
10 42 30.9	-59 25 41	-42.6	68
10 42 30.9	-59 24 10	-23.3	
10 42 30.9	-59 21 24	-33.6	
10 42 30.9	-59 21 20	-34.5	
10 42 31.0	-59 26 35	-40.7	69
10 42 31.0	-59 22 48	-21.0	
10 42 31.2	-59 23 5	-18.7	
10 42 31.2	-59 20 36	-38.4	66
10 42 31.2	-59 16 42	-17.2	
10 42 31.3	-59 29 27	-4.9	67
10 42 31.3	-59 26 35	-9.2	
10 42 31.6	-59 26 34	-10.6	69
10 42 31.6	-59 25 41	-9.0	68
10 42 31.9	-59 24 52	-44.9	70
10 42 32.1	-59 27 22	-36.7	71
10 42 32.2	-59 18 52	-5.8	
10 42 32.6	-59 27 21	-11.8	71
10 42 32.7	-59 24 54	-6.4	70
10 42 32.9	-59 25 14	-5.7	72
10 42 33.2	-59 19 17	-2.2	73
10 42 33.3	-59 25 17	-41.1	72
10 42 33.4	-59 21 38	-29.4	
10 42 33.6	-59 19 16	-28.2	73
10 42 33.7	-59 22 16	-33.1	
10 42 33.8	-59 18 3	-19.9	
10 42 33.8	-59 16 26	-19.7	
10 42 33.9	-59 24 25	-23.6	
10 42 34.1	-59 28 9	-42.0	74
10 42 34.2	-59 23 4	-19.8	
10 42 34.3	-59 24 8	-25.8	
10 42 34.3	-59 19 54	-7.8	75
10 42 34.5	-59 29 11	-8.3	
10 42 34.7	-59 28 7	-7.5	74
10 42 34.7	-59 23 17	-17.7	
10 42 34.7	-59 19 54	-25.7	75
10 42 35.0	-59 21 27	-29.7	
10 42 35.0	-59 20 35	-18.4	
10 42 35.3	-59 25 30	-4.9	76
10 42 35.6	-59 26 31	-43.5	77
10 42 35.6	-59 25 44	-42.9	78
10 42 35.8	-59 25 32	-42.6	76
10 42 35.9	-59 18 42	-12.6	
10 42 36.1	-59 21 57	-27.7	
10 42 36.2	-59 16 11	-18.1	
10 42 36.3	-59 25 44	-7.7	78
10 42 36.4	-59 26 31	-8.6	77
10 42 36.5	-59 25 1	-41.9	79
10 42 36.6	-59 27 14	-40.0	80
10 42 36.7	-59 24 39	-20.4	
10 42 37.0	-59 17 51	-20.2	
10 42 37.2	-59 27 13	-9.5	80
10 42 37.3	-59 25 3	-5.1	79
10 42 37.3	-59 22 24	-26.0	
10 42 37.4	-59 28 57	-44.7	81
10 42 37.4	-59 20 37	-26.8	
10 42 37.4	-59 19 8	-35.4	
10 42 37.7	-59 25 44	-5.1	82
10 42 37.9	-59 23 28	-17.5	
10 42 37.9	-59 23 22	-11.1	
10 42 38.0	-59 25 47	-37.1	82
10 42 38.1	-59 28 53	-6.4	81
10 42 38.2	-59 19 49	-10.5	
10 42 38.3	-59 27 55	-43.1	83
10 42 38.7	-59 24 22	-22.2	
10 42 38.7	-59 21 31	-27.9	
10 42 38.9	-59 20 33	-20.6	
10 42 39.0	-59 27 53	-8.2	83
10 42 39.0	-59 22 17	-22.5	
10 42 39.2	-59 18 32	-11.4	
10 42 39.5	-59 24 53	-35.7	
10 42 39.6	-59 20 58	-17.9	
10 42 40.0	-59 17 39	-19.9	
10 42 40.4	-59 19 1	-5.6	
10 42 40.7	-59 22 30	-20.4	
10 42 40.8	-59 26 28	-46.6	84
10 42 40.9	-59 25 47	-41.7	85
10 42 41.0	-59 23 39	-20.5	
10 42 41.2	-59 28 37	-46.4	86
10 42 41.6	-59 21 18	-28.7	
10 42 41.6	-59 19 45	-5.2	87
10 42 41.7	-59 25 48	-10.1	85
10 42 41.7	-59 23 40	-19.4	
10 42 41.8	-59 26 27	-6.2	84
10 42 41.9	-59 25 11	-30.6	
10 42 42.0	-59 28 33	-5.4	86
10 42 42.0	-59 25 5	-35.6	
10 42 42.1	-59 22 39	-19.2	
10 42 42.1	-59 19 44	-36.9	87
10 42 42.3	-59 21 34	-27.0	
10 42 42.3	-59 18 23	-9.5	
10 42 42.4	-59 29 35	-3.7	
10 42 42.5	-59 20 32	-22.7	
10 42 42.6	-59 27 2	-6.9	
10 42 42.7	-59 17 29	-11.8	
10 42 43.1	-59 27 39	-46.5	88
10 42 43.4	-59 24 37	-35.0	
10 42 43.6	-59 18 54	-6.2	
10 42 43.7	-59 22 37	-6.9	89
10 42 43.9	-59 23 48	-18.6	
10 42 44.1	-59 27 36	-6.3	88
10 42 44.1	-59 22 37	-35.6	89
10 42 44.1	-59 21 41	-23.7	
10 42 45.2	-59 18 15	-5.9	
10 42 45.3	-59 29 14	-39.8	90
10 42 45.5	-59 23 3	-19.9	
10 42 45.5	-59 21 36	-21.7	
10 42 45.8	-59 29 10	-6.7	90
10 42 45.8	-59 28 15	-43.2	
10 42 45.9	-59 20 31	-25.7	
10 42 46.0	-59 24 1	-32.7	91
10 42 46.4	-59 19 55	-8.0	
10 42 46.5	-59 24 4	-8.8	91
10 42 46.5	-59 22 5	-33.2	92
10 42 46.6	-59 23 57	-13.7	93
10 42 46.6	-59 18 48	-2.4	
10 42 46.8	-59 23 58	-35.6	93
10 42 46.8	-59 22 43	-8.8	94
10 42 46.9	-59 22 9	-2.5	92
10 42 47.2	-59 26 23	-45.7	95
10 42 47.2	-59 22 44	-38.3	94
10 42 47.5	-59 25 51	-38.2	
10 42 47.8	-59 26 52	-48.2	96
10 42 47.8	-59 20 17	-20.7	
10 42 47.9	-59 25 22	-42.7	
10 42 48.1	-59 19 35	-10.4	
10 42 48.4	-59 18 7	2.9	
10 42 48.6	-59 26 22	-4.2	95
10 42 48.6	-59 21 39	-21.3	
10 42 49.0	-59 20 30	-26.5	
10 42 49.1	-59 28 46	-40.6	97
10 42 49.2	-59 26 49	-4.9	96
10 42 49.4	-59 24 56	-34.7	
10 42 49.4	-59 23 31	-21.8	
10 42 49.4	-59 22 33	-34.6	98
10 42 49.4	-59 20 40	-29.7	
10 42 49.8	-59 28 42	-6.2	97
10 42 49.8	-59 22 37	-7.6	98
10 42 50.5	-59 27 15	-1.7	
10 42 51.2	-59 27 48	-42.6	99
10 42 51.2	-59 21 6	-28.4	
10 42 51.7	-59 21 42	-27.7	
10 42 52.0	-59 20 29	-28.6	
10 42 52.4	-59 27 41	.7	99
10 42 52.7	-59 23 5	-33.7	100
10 42 53.1	-59 21 35	-24.8	
10 42 53.2	-59 29 13	-38.2	101
10 42 53.8	-59 29 7	-1.9	101
10 42 53.8	-59 28 13	-44.5	102
10 42 54.0	-59 24 4	-32.0	103
10 42 54.2	-59 19 4	-22.9	
10 42 54.9	-59 28 5	1.2	102
10 42 55.1	-59 24 11	10.5	103
10 42 55.1	-59 22 5	-33.7	
10 42 56.3	-59 25 38	-49.4	104
10 42 56.7	-59 23 43	-38.1	
10 42 57.0	-59 28 34	-40.5	105
10 42 57.1	-59 25 20	-49.9	106
10 42 57.2	-59 20 18	-20.3	
10 42 57.5	-59 23 51	-.3	100
10 42 57.9	-59 28 25	.4	105
10 42 58.3	-59 20 45	-27.2	
10 42 58.6	-59 25 3	-47.0	107
10 42 58.9	-59 26 15	.9	
10 42 58.9	-59 25 58	.9	
10 42 59.1	-59 28 44	-40.7	108
10 42 59.2	-59 25 43	1.6	104
10 42 59.3	-59 26 30	2.6	
10 42 59.6	-59 21 15	-28.6	
10 42 59.8	-59 26 45	.6	
10 42 59.9	-59 28 35	-.6	108
10 43 0.0	-59 25 30	4.3	106
10 43 .2	-59 24 47	-48.9	109
10 43 .4	-59 27 26	-43.3	110
10 43 .5	-59 23 25	-39.7	111
10 43 .7	-59 27 0	-1.8	
10 43 .9	-59 21 48	-33.2	
10 43 1.1	-59 23 33	-4.4	111
10 43 1.3	-59 25 16	7.0	107
10 43 2.0	-59 24 35	-47.7	112
10 43 2.1	-59 27 13	-2.0	110
10 43 2.4	-59 27 39	-43.9	113
10 43 2.6	-59 25 4	7.3	109
10 43 2.6	-59 22 30	-20.4	
10 43 3.7	-59 27 46	-44.2	114
10 43 3.8	-59 27 24	-2.3	113
10 43 3.8	-59 24 53	2.8	112
10 43 4.4	-59 23 13	-39.7	115
10 43 4.6	-59 24 25	-44.7	116
10 43 4.7	-59 23 22	-4.2	115
10 43 4.9	-59 19 39	-10.5	
10 43 5.0	-59 27 30	-1.1	114
10 43 5.4	-59 20 6	-11.1	
10 43 5.8	-59 20 34	-14.9	
10 43 5.9	-59 24 44	3.6	116
10 43 6.1	-59 27 53	-41.7	117
10 43 6.4	-59 21 4	-27.3	
10 43 6.9	-59 21 39	-32.0	118
10 43 7.0	-59 27 36	-.2	117
10 43 7.0	-59 24 17	-46.2	119
10 43 7.0	-59 21 42	-13.7	118
10 43 7.6	-59 22 21	-24.0	
10 43 7.7	-59 24 35	-3.2	119
10 43 8.4	-59 23 6	-41.1	120
10 43 8.6	-59 23 16	-2.6	120
10 43 9.1	-59 24 17	4.1	
10 43 9.5	-59 24 12	-47.9	121
10 43 9.9	-59 24 33	-1.6	121
10 43 11.6	-59 24 32	-1.3	122
10 43 11.6	-59 24 12	-46.6	122
10 43 11.7	-59 23 15	-3.8	123
10 43 11.7	-59 23 6	-40.1	123
10 43 11.8	-59 22 20	-21.2	
10 43 11.8	-59 21 39	-22.9	
10 43 11.9	-59 21 4	-14.5	
10 43 12.0	-59 20 4	-7.0	
10 43 12.0	-59 19 36	-8.3	
10 43 12.1	-59 19 11	-5.0	
10 43 13.7	-59 24 34	-2.5	124
10 43 14.2	-59 24 16	-43.7	124
10 43 15.6	-59 23 19	-3.9	125
10 43 15.8	-59 24 38	-4.8	126
10 43 15.8	-59 23 9	-42.1	125
10 43 16.6	-59 24 22	-44.2	126
10 43 16.8	-59 22 28	-3.3	127
10 43 17.0	-59 22 21	-37.2	127
10 43 17.6	-59 24 47	-2.6	128
10 43 17.9	-59 21 45	-14.4	129
10 43 18.0	-59 21 42	-33.6	129
10 43 18.7	-59 24 52	-2.5	130
10 43 18.7	-59 21 11	-10.1	
10 43 18.9	-59 24 30	-45.1	128
10 43 19.2	-59 23 29	4.4	131
10 43 19.5	-59 20 39	-8.3	
10 43 19.8	-59 23 18	-41.4	131
10 43 20.1	-59 24 38	-41.9	130
10 43 20.2	-59 25 3	-2.6	132
10 43 20.3	-59 25 2	-4.2	
10 43 21.5	-59 25 16	-.6	
10 43 21.7	-59 22 39	-3.1	133
10 43 21.9	-59 24 51	-41.4	132
10 43 22.0	-59 22 33	-37.4	133
10 43 22.7	-59 23 42	1.4	134
10 43 23.4	-59 23 32	-43.1	134
10 43 23.6	-59 22 0	-3.7	135
10 43 23.9	-59 21 54	-39.2	135
10 43 24.6	-59 23 51	-.6	136
10 43 25.3	-59 21 25	-6.8	137
10 43 25.5	-59 23 42	-43.6	136
10 43 25.5	-59 21 22	-29.7	137
10 43 26.1	-59 22 57	.6	138
10 43 26.7	-59 22 49	-42.1	138
10 43 26.8	-59 20 55	-7.5	
10 43 27.5	-59 24 10	-2.3	139
10 43 28.1	-59 20 28	-4.2	
10 43 28.5	-59 24 3	-41.8	139
10 43 28.6	-59 23 10	2.3	140
10 43 29.0	-59 22 20	-5.3	141
10 43 29.3	-59 23 3	-40.2	140
10 43 29.4	-59 22 15	-39.7	141
10 43 29.4	-59 20 3	-1.3	
10 43 29.9	-59 24 34	-1.6	142
10 43 30.5	-59 19 39	.1	
10 43 31.0	-59 24 28	-41.9	142
10 43 31.4	-59 21 49	-7.0	
10 43 31.9	-59 22 36	-2.5	143
10 43 32.4	-59 23 35	-2.0	144
10 43 32.4	-59 22 31	-37.1	143
10 43 33.1	-59 23 30	-38.9	144
10 43 33.6	-59 21 21	-5.2	
10 43 34.8	-59 22 6	-4.7	145
10 43 35.2	-59 22 2	-37.2	145
10 43 35.5	-59 20 55	-6.6	
10 43 36.4	-59 23 6	-3.2	146
10 43 37.0	-59 23 2	-39.5	146
10 43 37.4	-59 21 40	-7.7	
10 43 39.9	-59 22 41	-5.1	147
10 43 40.4	-59 22 37	-40.2	147
10 43 43.0	-59 22 19	-7.2	
10 43 45.8	-59 21 58	-9.6	

Table 3. Radial velocities (to within an additive constant) obtained from [N II] line

α_{1950}	δ_{1950}	V_{LSR} km/s	α_{1950}	δ_{1950}	V_{LSR} km/s	α_{1950}	δ_{1950}	V_{LSR} km/s
10 42 39.5	-59°23 54	-24.5	10 42 48.3	-59 22 53	-45.7	10 42 55.5	-59°22 27	-38.2
10 42 40.0	-59 26 22	-14.9	10 42 48.3	-59 21 49	-13.9	10 42 56.2	-59 24 7	-42.9
10 42 40.8	-59 23 14	-26.3	10 42 48.6	-59 23 45	-37.1	10 42 57.0	-59 24 3	-40.9
10 42 41.2	-59 24 0	-27.5	10 42 48.6	-59 23 36	-15.7	10 42 58.6	-59 22 42	-19.0
10 42 41.3	-59 25 3	-39.5	10 42 48.7	-59 22 42	-46.2	10 42 59.1	-59 22 56	-37.8
10 42 41.5	-59 22 39	-29.7	10 42 48.8	-59 23 56	-39.9	10 42 59.4	-59 23 5	-12.0
10 42 41.6	-59 24 0	-22.8	10 42 48.9	-59 22 21	-7.8	10 42 59.8	-59 23 17	-43.6
10 42 41.8	-59 26 17	-16.0	10 42 49.0	-59 23 6	-12.9	10 43 .3	-59 23 32	-8.4
10 42 42.1	-59 26 52	-12.7	10 42 49.0	-59 22 45	-9.0	10 43 .7	-59 23 43	-48.3
10 42 42.2	-59 22 23	-26.8	10 42 49.1	-59 21 55	-49.2	10 43 .7	-59 22 22	-13.3
10 42 42.5	-59 25 1	-37.5	10 42 49.3	-59 21 31	-43.2	10 43 1.0	-59 22 37	-22.8
10 42 43.1	-59 24 5	-31.9	10 42 49.5	-59 23 17	-14.7	10 43 1.3	-59 22 52	-40.7
10 42 43.1	-59 23 15	-27.4	10 42 49.6	-59 22 50	-45.2	10 43 1.5	-59 22 28	-11.8
10 42 43.3	-59 23 29	-24.8	10 42 49.7	-59 23 12	-47.9	10 43 1.5	-59 22 9	-40.4
10 42 43.4	-59 22 43	-36.3	10 42 49.8	-59 23 43	-14.0	10 43 1.5	-59 21 43	-31.6
10 42 43.5	-59 23 56	-29.2	10 42 49.8	-59 22 25	-48.5	10 43 1.6	-59 23 12	-47.0
10 42 43.6	-59 25 4	-40.4	10 42 49.9	-59 23 43	-40.9	10 43 1.9	-59 23 28	-11.2
10 42 43.7	-59 26 44	-15.5	10 42 50.0	-59 22 56	-14.0	10 43 5.0	-59 23 28	-8.5
10 42 43.8	-59 26 11	-17.5	10 42 50.0	-59 21 37	-14.2	10 43 5.2	-59 23 11	-47.3
10 42 43.9	-59 21 58	-27.8	10 42 50.1	-59 24 28	-41.1	10 43 5.3	-59 23 0	-14.4
10 42 44.0	-59 23 55	-17.0	10 42 50.3	-59 22 58	-10.3	10 43 5.4	-59 22 49	-43.8
10 42 44.0	-59 22 28	-38.5	10 42 50.4	-59 24 19	-39.5	10 43 5.4	-59 22 37	-13.7
10 42 44.1	-59 24 53	-40.3	10 42 50.5	-59 22 48	-12.2	10 43 5.6	-59 22 33	-34.0
10 42 44.2	-59 22 44	-13.6	10 42 50.5	-59 22 4	-9.1	10 43 5.8	-59 22 14	-38.0
10 42 44.7	-59 22 31	-17.0	10 42 50.6	-59 23 19	-12.8	10 43 6.0	-59 22 31	-23.6
10 42 44.8	-59 23 12	-25.8	10 42 50.8	-59 23 49	-14.3	10 43 6.7	-59 22 24	-38.5
10 42 44.8	-59 21 25	-23.3	10 42 50.8	-59 21 44	-46.5	10 43 6.8	-59 23 45	-4.3
10 42 45.0	-59 23 37	-29.9	10 42 51.1	-59 23 6	-38.4	10 43 7.5	-59 23 32	-5.9
10 42 45.1	-59 24 12	-35.0	10 42 51.2	-59 24 8	-44.1	10 43 7.7	-59 22 46	-20.4
10 42 45.3	-59 23 38	-19.3	10 42 51.3	-59 23 17	-49.0	10 43 8.1	-59 23 15	-48.7
10 42 45.5	-59 22 47	-45.7	10 42 51.3	-59 22 10	-49.0	10 43 8.5	-59 23 5	-16.0
10 42 45.5	-59 22 5	-39.5	10 42 51.4	-59 23 26	-47.7	10 43 8.5	-59 23 4	-13.2
10 42 45.7	-59 26 35	-12.0	10 42 51.6	-59 22 34	-10.6	10 43 8.7	-59 22 41	-36.3
10 42 45.9	-59 24 43	-40.3	10 42 51.8	-59 21 53	-10.8	10 43 8.8	-59 22 1	-32.8
10 42 45.9	-59 23 51	-32.6	10 42 51.9	-59 23 13	-8.5	10 43 9.3	-59 22 43	-15.5
10 42 45.9	-59 23 15	-22.0	10 42 52.0	-59 23 39	-43.0	10 43 9.9	-59 24 24	-8.8
10 42 45.9	-59 22 34	-48.2	10 42 52.2	-59 23 58	-43.3	10 43 10.2	-59 22 22	-30.6
10 42 46.2	-59 25 5	-41.2	10 42 52.2	-59 23 1	-42.2	10 43 10.7	-59 22 8	-23.5
10 42 46.2	-59 21 35	-26.1	10 42 52.5	-59 23 36	-11.2	10 43 11.6	-59 22 25	-28.8
10 42 46.3	-59 22 9	-15.1	10 42 52.7	-59 23 21	-39.3	10 43 12.1	-59 24 44	-12.4
10 42 46.7	-59 23 49	-13.2	10 42 52.7	-59 22 54	-39.7	10 43 13.1	-59 24 0	-4.4
10 42 46.7	-59 23 45	-36.8	10 42 52.9	-59 22 4	-38.5	10 43 13.8	-59 22 13	-18.8
10 42 46.8	-59 23 24	-14.5	10 42 53.1	-59 22 22	-6.6	10 43 15.9	-59 22 2	-16.0
10 42 46.8	-59 22 50	-13.7	10 42 53.5	-59 24 2	-42.0	10 43 16.3	-59 24 32	-11.3
10 42 47.3	-59 22 14	-49.2	10 42 53.5	-59 23 44	-46.7	10 43 17.8	-59 21 52	-15.0
10 42 47.4	-59 24 19	-38.2	10 42 53.6	-59 24 38	-43.9	10 43 19.4	-59 24 22	-10.8
10 42 47.4	-59 22 38	-13.2	10 42 53.6	-59 23 30	-8.0	10 43 19.5	-59 21 43	-16.7
10 42 47.5	-59 23 49	-12.8	10 42 53.7	-59 22 43	-36.7	10 43 21.0	-59 21 35	-14.0
10 42 47.5	-59 22 53	-12.0	10 42 54.0	-59 22 13	-9.5	10 43 22.0	-59 24 14	-10.1
10 42 47.6	-59 21 44	-40.0	10 42 54.3	-59 25 7	-25.8	10 43 22.5	-59 21 27	-16.2
10 42 47.9	-59 24 32	-40.7	10 42 54.3	-59 23 37	-47.7	10 43 22.5	-59 22 37	-12.0
10 42 48.1	-59 21 20	-30.6	10 42 54.4	-59 24 23	-45.1	10 43 24.1	-59 24 8	-6.9
10 42 48.2	-59 22 59	-45.1	10 42 54.6	-59 22 33	-39.0	10 43 24.4	-59 22 33	-11.2
10 42 48.3	-59 23 15	-34.9	10 42 55.1	-59 24 16	-44.6	10 43 26.2	-59 24 1	-9.2

plained by Dyson's globule model (Dyson, 1968a, 1968b). A fortiori, Dyson's model cannot explain this larger scale splitting.

To explain both the velocity difference between the ionized gas and the molecules, and the molecular velocity gradient, Dickel (1974) suggests an expanding shell model. Highly compressed neutral gas surrounds an H II region and expands. From our results, the presence of two clouds of ionized gas along the line of sight over most of the nebula strongly reinforces the explanation by a shell model; the shell of ionized gas should be empty near its center.

In Fig. 8, we have plotted the difference ΔV of radial velocities between the two components of the line, versus the distance ϱ to the expansion centre given by Dickel (1974). This difference should vary as $2V_E \cos\theta$, where V_E is the expansion velocity of a spherical shell, and θ the angle between the line of sight and the radius vector to the point on the shell; we find no such correlation between ΔV and ϱ. This disagreement could be due to the following reasons:

— a spherical nebula is certainly too schematic to represent a complicated structure.

— the determination of parameters such as the position of the expansion centre may be inaccurate because of the large beamwidths of molecular observations.

As the largest splitting is obtained near the star η Carinae, we have chosen this star as center of expansion. In Fig. 9 we have plotted the radial velocities V_{LSR} versus the distance ϱ to η Carinae, for a sector of the nebula. Figure 9 shows that the difference between the velocities of the two components of Hα decreases

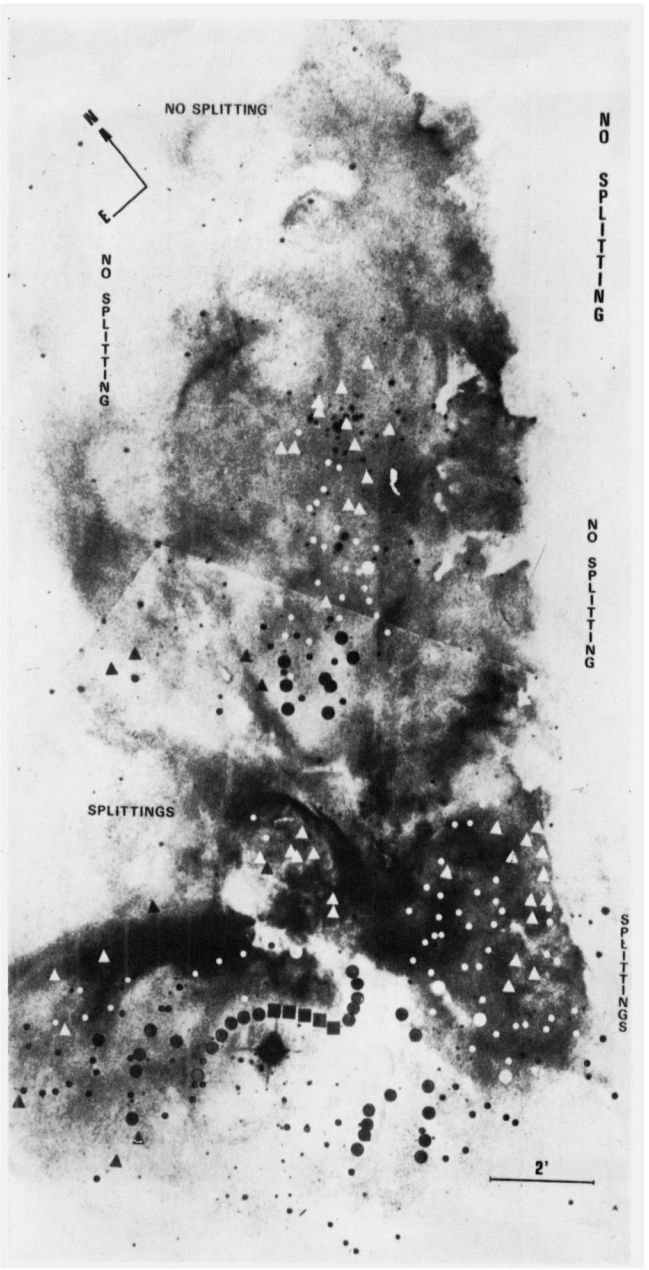

Fig. 6. Hα splitting: squares: the difference ΔV between the velocities of the two components of the line is greater than 50 km s^{-1}; large circles (black or white): 50 km s^{-1} $\geqslant \Delta V >$ 40 km s^{-1}; small circles (black or white): 40 km s^{-1} $\geqslant \Delta V >$ 30 km s^{-1}; triangles (black or white) $\Delta V \leqslant$ 30 km s^{-1}

uniformly with increasing distance from the star. At $\varrho = 20'$, no splitting is observed; the velocities converge to the mean between the velocities of the two components.

The investigation in this sector of the nebula shows that this region is in expansion, with a velocity $V_E \geqslant 25$ km s^{-1}. Furthermore, Fig. 6 shows that the expansion possesses non-spherical symmetry; the difference between the velocities of the two components of Hα decreases more strongly in some directions than in others.

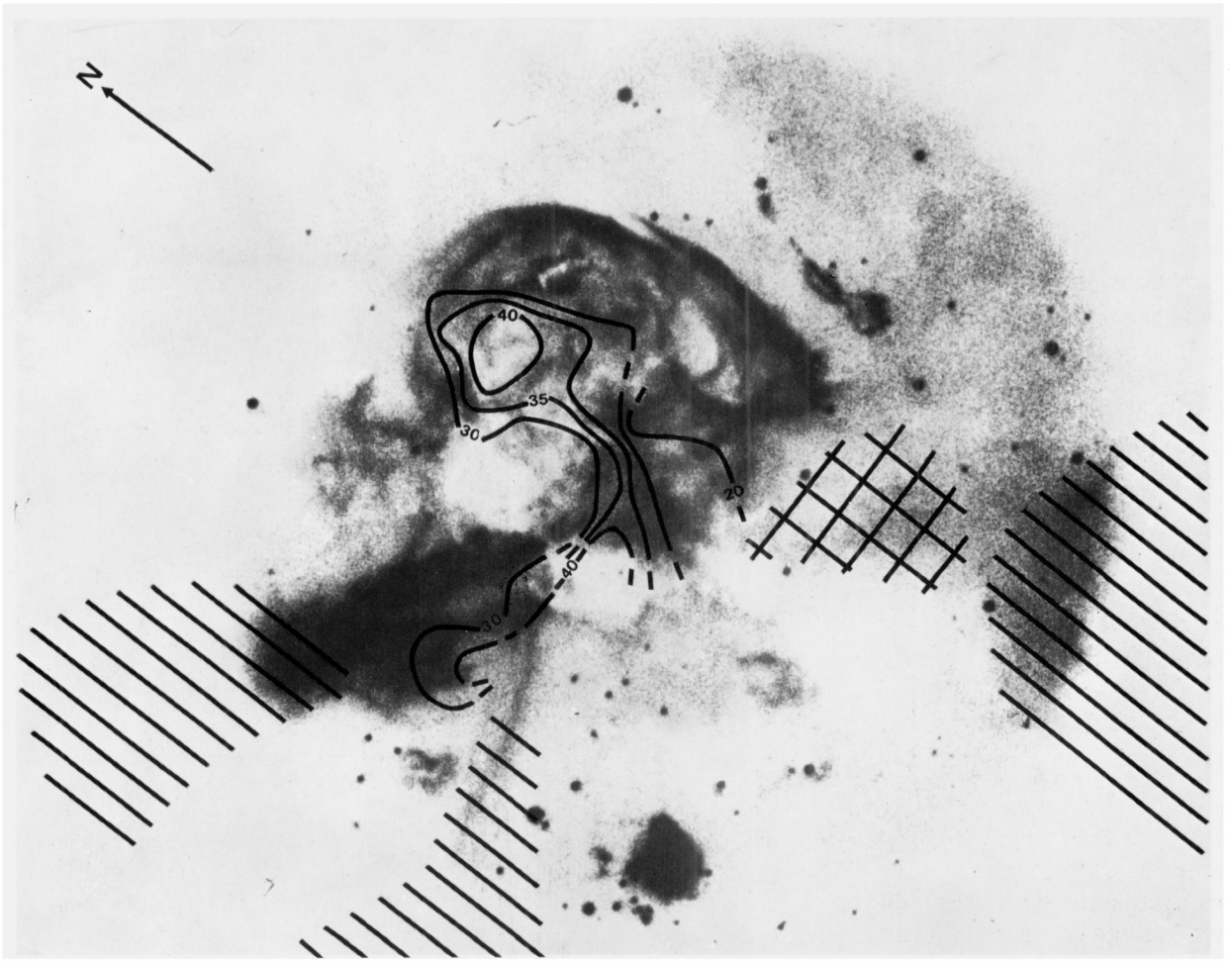

Fig. 7. [N II] splitting; the differences between the velocities of the components of the line are indicated in km s^{-1}: in the lined region, only a receding emitting cloud is observed, while only an approaching one is found in the cross-hatched region

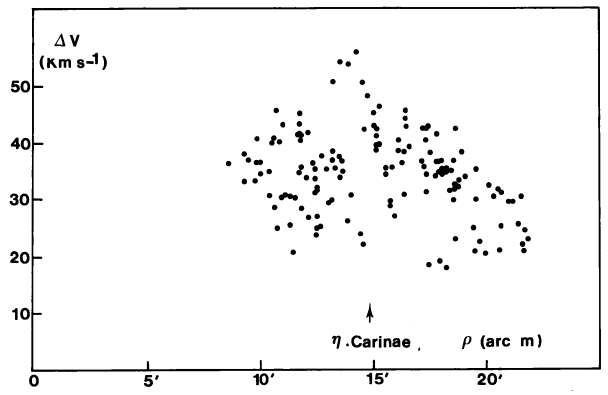

Fig. 8. For each Hα splitting, we plot the difference between the velocities of each component of the line, versus the distance to the centre of expansion given by Dickel (1974)

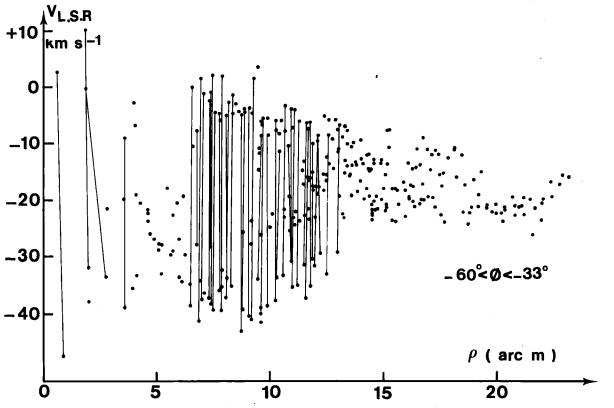

Fig. 9. Radial velocity versus distance from the star η Carinae, for one sector of the nebula; Φ is the angle between the selected directions and the north. The points connected by a line correspond to two components of Hα

IV. Conclusion

Our results concerning the kinematics of the ionized gas are in very good agreement with those obtained from radio observations.

The existence of expansion inside the Carina Nebula, suggested by Dickel from molecular observations, is confirmed by our results concerning the ionized gas. Nevertheless this expansion appears to have a non-spherical symmetry and the expansion velocity ($\geqq 25$ km s^{-1}) is larger than that given by Dickel (7 km s^{-1}). This is not so puzzling because molecular and H II observations do not refer to the same regions

of the nebula (respectively the outer, approaching, neutral region, and the inner ionized gas). Furthermore, the center of expansion seems to be associated with the peculiar star η Carinae (in disagreement with the center of expansion given by Dickel).

Nevertheless, it is difficult to understand how the picture of an expanding shell, obtained from results concerning the kinematics of the neutral and ionized gas, and the picture of a two-peaked nebula obtained from observations in the radio-continuum, can describe the same object. Radio observations in the continuum, with a better angular resolution, are very much needed to resolve this problem.

Acknowledgements. ESO organisation is gratefuly acknowledged for observing time and for permission to reproduce a Schmidt plate in Fig. 1. This reproduction was kindly supplied by Dr. West. Thanks are also due to J. M. Deharveng for taking several photographs of the Nebula, J. Caplan, G. Courtès, P. Cruvellier, Y. P. Georgelin, and G. Monnet for helpful discussions.

References

Courtès, G. 1960, *Ann. Astrophys.* **23**, 115
Deharveng, L. 1973, *Astron. & Astrophys.* **29**, 341
Dickel, H. R., Wall, J. V. 1974, *Astron. & Astrophys.* **31**, 5
Dickel, H. R. 1974, *Astron. & Astrophys.* **31**, 11
Dyson, J. E. 1968a, *Astrophys. Space Sci.* **1**, 388
Dyson, J. E. 1968b, *Astrophys. Space Sci.* **2**, 461
Faulkner, D. J. 1963, *Publ. Astron. Soc. Pacific* **75**, 269
Faulkner, D. J., Aller, L. H. 1965, *Monthly Notices Roy. Astron. Soc.* **130**, 393
Gardner, F. F., Morimoto, M. 1968, *Australian J. Phys.* **21**, 881
Gardner, F. F., Milne, D. K., Mezger, P. G., Wilson, T. L. 1970, *Astron. & Astrophys.* **7**, 349
Georgelin, Y. P. 1969, Thesis, University of Aix-Marseille
Hoffman, W. F., Frederick, C. L., Emery, R. J. 1973, *Bull. Am. Astron. Soc.* **5**, 31
McGee, R. X., Gardner, F. F. 1968, *Australian J. Phys.* **21**, 149
McGee, R. X., Batchelor, R. A., Brooks, J. W., Sinclair, M. W. 1969, *Australian J. Phys.* **22**, 631
Pottasch, S. R. 1956, *Bull. Astron. Inst. Neth.* **13**, No. 471, 77
Pottasch, S. R. 1965, *Vistas Astron.* **6**, 149
Shaver, P. A., Goss, W. M. 1970, *Australian J. Phys. Suppl.* **14**, 77
Sher, D. 1965, *Quart. J. Roy. Astron. Soc.* **6**, 299
Smith, M. G. 1970, *Trans.* IAU, XIV B, Commission **34**
Smith, M. G. 1972, *Astron. & Astrophys.* **16**, 482
Walborn, N. R. 1971, *Astrophys. J.* **167**, L 31
Walborn, N. R. 1973, *Astrophys. J.* **179**, 517
Wilson, T. L., Mezger, P. G., Gardner, F. F., Milne, D. K. 1970, *Astron. & Astrophys.* **6**, 364

L. Deharveng
Observatoire de Marseille
2, Place Le Verrier
F-13004 Marseille, France

M. Maucherat
Laboratoire Astronomie Spatiale
Traverse du Siphon
Les Trois Lucs
F-13012 Marseille, France